Hindawi
Journal of Electrical and Computer Engineering
Volume 2022, Article ID 4932284, 11 pages
https://doi.org/10.1155/2022/4932284

Research Article

Design of Electronically Controllable Multifunction Active Filter with Amplitude Controllability Using Two Commercially Available ICs

Narumol Onanong,[1] Piya Supavarasuwat,[1] Daungkamol Angamnuaysiri,[2] Surapong Siripongdee,[1] Amornchai Chaichana,[1] Winai Jaikla,[1] and Peerawut Suwanjan[1]

[1]*Department of Engineering Education, School of Industrial Education and Technology, King Mongkut's Institute of Technology Ladkrabang, Bangkok 10520, Thailand*
[2]*Program of Robot and Smart Electronics Engineering, Faculty of Engineering and Industrial Technology, Phetchaburi Rajabhat University, Phetchaburi 76000, Thailand*

Correspondence should be addressed to Piya Supavarasuwat; piya.su@kmitl.ac.th

Received 12 April 2022; Revised 13 June 2022; Accepted 16 July 2022; Published 4 August 2022

Academic Editor: Raj Senani

In this contribution, the design and analysis of an active multifunction biquad filter that provides five voltage-mode filtering configurations in the same core filtering circuit are presented. The design emphasizes using the commercially available ICs, LT1228, which are easy for off-the-shelf implementation and cheaper compared with the chip implementation. The proposed multifunction filter is realized from two commercial LT1228 ICs as the active function block, combined with five passive elements (three resistors and two capacitors) with three input voltage nodes and a single output voltage node. The following advantages are given for this design: (i) it provides high-pass (HP), low-pass (LP), band-stop (BS), band-pass (BP), and all-pass (AP) filtering functions; (ii) orthogonal and electronic tuning of the natural frequency (ω_0) and bandwidth (the quality factor: Q); (iii) output voltage node of the proposed circuit is low impedance; (iv) passband voltage gain is controllable; and (v) matching condition and extra double gain voltage-mode amplifier are not required. The effect of the parasitic element in LT1228 on the filter performance is analyzed and included to strengthen the design idea. The PSpice simulation results using LT1228 with ±5 V and the experimental results tested from the hardware implementation are given to prove the validity of the designed multifunction filter.

1. Introduction

Filters are one of the most important circuits in analog signal processing systems. They are used extensively in many fields, such as electronics, communication systems, control systems, measurement systems, and instrumentation [1]. It can be said that most of the electronic devices in the above works have filters as part of the circuit. For this reason, the filter circuit is continuously developed, researched, and implemented. In particular, a frequency filter that can provide several responses or multiple functions in the same circuit structure has received a lot of attention [2–6]. It is called a multifunction filter circuit. The design of an analog active multifunction filter in the category of multiple-input single-output (MISO) type continues to gain popularity [7, 8]. This is due to the filtering functions, high-pass (HP), low-pass (LP), band-stop (BS), band-pass (BP), and all-pass (AP), which can be selected by controlling on or off the input signals at the input voltage nodes. This feature can be controlled by the digital approach by employing a microcontroller or microprocessor. The voltage-mode analog active filters are always designed to obtain a low-output impedance feature, which makes it convenient to connect with other circuits without the need for buffers. In addition, the filtering parameters should be able to control by an electronic method. Nowadays, electronic devices tend to use

a microcontroller or microprocessor to control all functions of these devices. Nevertheless, the MISO voltage-mode filtering topology necessitates reconnection of the inputs once a specific input must be grounded, and another port must be disconnected from ground to be used as a new voltage input. Solely voltage-mode filtering solutions with a single input and a single output (SIMO) can be referred to as "no-reconnect" solutions. In exchange, a low-impedance node lacks a voltage response.

Electronic circuit design using active building blocks (ABBs) is very popular. As it provides a great deal of convenience and flexibility for designers, the circuits designed using active building blocks are simple in structure and often contain a few passive devices [9–11]. Currently, there are a variety of active building blocks with bipolar junction transistor structures or C-MOS transistor structures. Its advantage is that it can operate at a low power supply and low power consumption. In addition, the transistor level-based circuits can work at high frequencies as well. However, the circuits realized at the transistor level are most efficient when they are fabricated into an integrated circuit. The cost of fabricating an integrated circuit into a chip is also expensive. For these reasons, it is always found that the performance of the circuits realized at the transistor or C-MOS level will be verified through simulation only due to cost reasons. In addition, the implementation of circuits into the chip should be manufactured in large quantities to achieve break-even. Therefore, using the commercially available active building blocks to realize the new active circuits with a few amounts for specific applications is more interesting and cheaper. It can be easily purchased commercially ICs in the electronic market. It is also easy to implement cheap circuits for real performance testing [12–14]. An interesting commercial active building block is the LT1228. An LT1228 has an internal structure that consists of the operational transconductance amplifier (OTA) and the current feedback amplifier (CFA). So, it can be used in a variety of applications, such as being used in voltage-mode circuit design, where the output terminal is low impedance, and the input terminals are high impedance. It is also electronically controllable, making it easy to control circuit operations with a microcontroller or microprocessor.

According to the study, the MISO multifunction active filters employing various active building blocks have been presented [15–44]. However, those studies may still have some disadvantages. For example, the ABB is not easily realized from the commercially available ICs [15, 22, 26, 27, 29–34, 36, 40–43]; the filtering parameters are not controlled electronically [17–21, 24–32, 34, 35]; the output impedance node is not low [15, 16, 18–23, 29, 30, 32–37, 40–44]; the matching condition is needed for selecting the filtering functions [20, 28, 31–34, 42, 43]; the extra double gain amplifier is needed [33, 41, 43, 44], and the performance of the proposed multifunction active filters is verified through simulation only [15, 16, 19, 22, 24, 26, 27, 29–34, 36, 37, 40–44]; the quality factor cannot be controlled without affecting the natural frequency [15–38, 40–42, 44]; and the passband gain of the proposed filters cannot be controlled [15–30, 32–44]. The comparison of the proposed commercially available IC-based MISO multifunction active filter and others is given in Table 1.

For the reasons presented above, a commercially available LT1228 IC-based multifunction active filter is proposed in this research paper. The rest of this research contribution is prepared as follows: the basic concept of the commercially available LT1228 IC and the proposed voltage-mode MISO multifunction active filter are given in Section 2, while Section 3 presents, in detail, the analysis and study of the effect of the parasitic impedances in LT1228. The simulation results obtained from the PSpice program are depicted in Section 4. In Section 4, the experimental results obtained from the real circuit test are shown and discussed. Finally, the conclusion of this study is depicted in Section 5.

2. Principle of the Proposed Circuit

2.1. Active Building Block and Its Properties. The commercially available LT1228 IC is a voltage input and current/voltage output active building block that consists of a cascading connection of the transconductance amplifier and the current feedback amplifier [45, 46]. It has five terminals where v_+ and v_- are the high-impedance (ideally infinity) voltage input terminals. The y is a high-impedance (ideally infinity) current output terminal of the transconductance amplifier, and this terminal is also the voltage input terminal of the current feedback amplifier section. The low-impedance (ideally zero) terminals x and w in LT1228 are the voltage input and output of the current feedback amplifier, respectively. The LT1228 electrical circuit symbol is depicted in Figure 1(a), while the equivalent circuit of LT1228 is shown in Figure 1(b). The pin configuration of the LT1228 is an 8-pin dual-in-line package IC as shown in Figure 2. The LT1228 terminal characteristics are presented in the following equation [46]:

$$\begin{pmatrix} I_{v+} \\ I_{v-} \\ I_y \\ V_x \\ V_w \end{pmatrix} = \begin{pmatrix} 0 & 0 & 0 & 0 & 0 \\ 0 & 0 & 0 & 0 & 0 \\ g_m & -g_m & 0 & 0 & 0 \\ 0 & 0 & 1 & 0 & 0 \\ 0 & 0 & 0 & R_T & 0 \end{pmatrix} \begin{pmatrix} V_+ \\ V_- \\ V_y \\ I_x \\ I_w \end{pmatrix}, \tag{1}$$

where R_T denotes the transresistance gain of LT1228 and g_m denotes the transconductance gain. For ideal consideration, R_T is an infinite value. g_m of LT1228 depends on the DC bias current I_B as depicted in the following equation [46]:

$$g_m = 10I_B. \tag{2}$$

Equation (2) indicates that the LT1228-based circuits are electronically tuned, which makes it easy to control circuit parameters with a microcontroller or microprocessor.

2.2. Proposed Multifunction Active Filter. This design focuses on employing the LT1228 IC to obtain the electronic control of the natural frequency and bandwidth (the quality factor), which will be easy for off-the-shelf implementation and

Table 1: Comparison of this MISO multifunction active filter and other works.

Ref	ABB	No. of ABB	No. of $R+C$	All grounded passive elements	Commercial IC	Electronic tune	Low output impedance	No need of matching condition	No need of double input	Experimental result	Control Q without affecting f_0	Passband gain control
15	OTA	6	0 + 2	Yes	Yes	Yes	No	Yes	Yes	No	No	No
16	OTA + CCII	3	0 + 2	No	Yes	Yes	No	Yes	Yes	No	No	No
17	CCII + VF	4	3 + 2	No	Yes	No	Yes	Yes	Yes	Yes	No	No
18	CCII	2	3 + 2	No	Yes	No	No	Yes	Yes	Yes	No	No
19	CCII	2	2 + 2	No	Yes	No	No	Yes	Yes	No	No	No
20	CCII	2	3 + 2	No	Yes	No	No	No	Yes	Yes	No	No
21	CCII	2	2 + 2	No	Yes	No	No	Yes	Yes	Yes	No	No
22	CCCII	2	0 + 2	No	No	Yes	No	Yes	Yes	No	No	No
23	CCTA	1*	2 + 2	No	Yes	Yes	No	Yes	Yes	Yes	Yes	No
24	CDBA	2*	4 + 2	No	Yes	No	Yes	Yes	Yes	No	Yes	No
25	CFA and VF	2	2 + 2	No	Yes	No	Yes	Yes	Yes	Yes	No	No
26	DDCC	2	2 + 2	No	No	No	Yes	Yes	Yes	No	No	No
27	DDCC	3	2 + 2	Yes	No	No	Yes	Yes	Yes	No	No	No
28	FTFN and CFA	2*	3 + 2	No	Yes	No	Yes	No	Yes	Yes	Yes	No
29	FDCCII	1	3 + 2	No	No	No	No	Yes	Yes	No	Yes	No
30	FDCCII	2	2 + 2	Yes	No	No	No	Yes	Yes	No	No	No
31	OTRA	1	4 + 4	No	No	No	Yes	No	Yes	No	No	Yes
32	DXCCII	1	4 + 2	No	No	No	No	No	Yes	No	Yes	No
33	VDTA	1	0 + 2	No	No	Yes	No	No	No	No	No	No
34	DVCC	1	2 + 2	No	No	No	No	No	Yes	No	No	No
35	CFA**	1	3 + 2	No	Yes	No	No	Yes	Yes	Yes	No	No
36	VD-DIBA	1	1 + 2	No	No	Yes	No	Yes	Yes	No	No	No
37	LT1228	1	1 + 2	No	Yes	Yes	No	Yes	Yes	No	No	No
38	VDDDA	2*	0 + 2	Yes	Yes	Yes	Yes	Yes	Yes	Yes	No	No
39	VDDDA	3*	0 + 2	Yes	Yes	Yes	Yes	Yes	Yes	Yes	Yes	No
40	VDDDA	1	2 + 2	No	Yes	Yes	No	Yes	Yes	No	Yes	No
41	VDDDA	1	1 + 2	No	Yes	Yes	No	Yes	No	No	No	No
42	VDTA	1	1 + 2	No	No	Yes	No	No	Yes	No	Yes	No
43	OTA	9	0 + 3	Yes	Yes	Yes	No	No	No	No	Yes	No
44	LT1228	1	2 + 2	No	Yes	Yes	No	Yes	No	No	Yes	No
This work	LT1228	2	3 + 2	No	Yes	Yes	Yes	Yes	Yes	Yes	Yes	Yes

*The CCTA in [23] is constructed from two commercial ICs, OPA861 and MAX435. The CDBA in [24] is structured from two commercial ICs of AD844. The FTFN in [28] is constructed from two commercial ICs of AD844. The VDDDA in [38, 39] is constructed from two commercial ICs, LT1228 and AD830. **In [35], reconnection of the proposed filter to obtain several filtering functions is required.

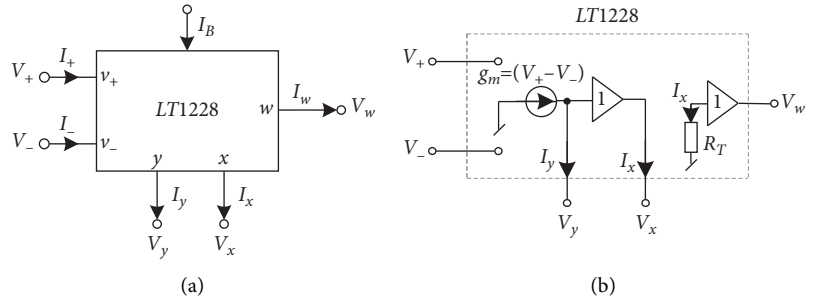

Figure 1: LT1228. (a) Electrical symbol. (b) Equivalent circuit.

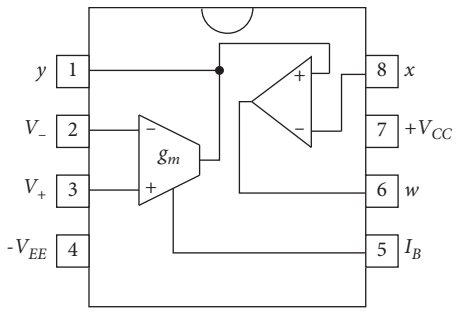

Figure 2: An 8-pin dual-in-line package of LT1228.

cheaper compared with the chip implementation. The presented multifunction active filter is depicted in Figure 3. It contains two LT1228 ICs (LT1228-1 and LT1228-2) as the main active building blocks with three resistors (R, R_a, and R_b) and two capacitors (C_1 and C_2). It has three input voltage nodes, V_{inI}, V_{in2}, and V_{in3}, and a single-output voltage node, V_0. Considering the proposed filter in Figure 3, the output voltage node, V_0, is at the w terminal of LT1228-2, which is low impedance. So, the output voltage node of the proposed active filter designed in Figure 3 can be directly connected to the next stage without using any voltage buffers. The input voltage node, V_{in3}, is also high impedance. However, the input voltage nodes, V_{in2} and V_{in1}, are not high impedance. Moreover, some passive elements in the proposed circuit are floating, which can be considered as the drawback when it is compared to the MISO filters proposed in [15, 27, 30, 38, 39, 43]. Considering the ideal properties of the LT1228, the equation of V_0 of the proposed circuit is obtained as follows:

$$v_o = \left(\frac{R_b}{R_a} + 1\right)\left(\frac{s^2 v_{in2} + \left(s g_{m2} v_{in3}/C_2\right) + \left(g_{m1} v_{in1}/C_1 C_2 R\right)}{s^2 + \left(s g_{m2}/C_2\right) + \left(g_{m1}/C_1 C_2 R\right)}\right). \tag{3}$$

Based on the denominator of equation (3), the natural frequency (ω_0) of the active filter designed in Figure 3 is obtained as follows:

$$\omega_0 = \sqrt{\frac{g_{m1}}{C_1 C_2 R}}. \tag{4}$$

Subsequently, the quality factor (Q) of the proposed multifunction active filter designed in Figure 3 is obtained as follows:

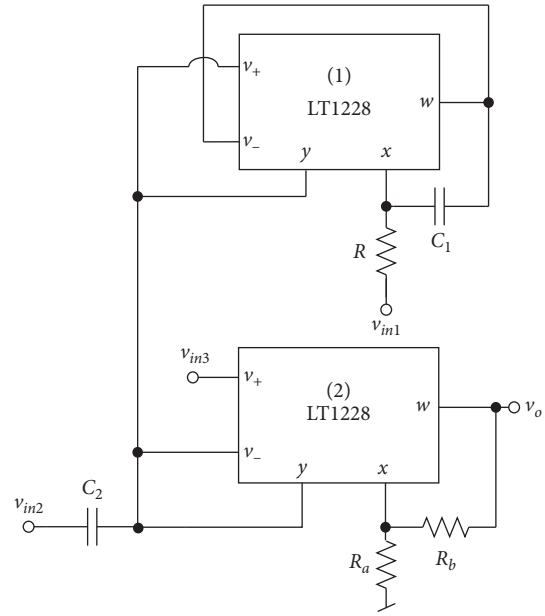

Figure 3: Proposed multifunction active filter.

$$Q = \frac{1}{g_{m2}} \sqrt{\frac{g_{m1} C_2}{R C_1}}. \tag{5}$$

The passband voltage gain of the proposed multifunction active filter designed in Figure 3 is given as follows:

$$G_p = \left(\frac{R_b}{R_a} + 1\right). \tag{6}$$

The filtering parameters, $\omega 0$ and Q, which appear in equations (4) and (5), indicate that the control of Q can be done electronically via the transconductance, g_{m2} of LT1228-2 without affecting $\omega 0$. Moreover, $\omega 0$ can be electronically adjusted via the transconductance, g_{m1} of LT1228-1. For practical design, $\omega 0$ should be first tuned electronically by g_{m1}, and then, the bandwidth or the Q should be electronically adjusted through g_{m2}. In addition, it is observed from equation (6) that the passband gain of all filtering functions can be controlled via the resistor, R_a or R_b, without affecting $\omega 0$ and Q. So, if the input magnitude signal driven to the proposed multifunction active filter is at a low level, the amplitude of the output voltage can be controlled without using any additional amplifiers.

Considering the output voltage depicted in (3), five second-order filtering functions can be achieved as follows:

(i) The band-pass biquad function can be realized from the proposed active filter designed in Figure 3 by driving the input voltage signal to node v_{in3} and connecting nodes v_{in1} and v_{in2} to the ground

(ii) The low-pass biquad function can be realized from the proposed active filter designed in Figure 3 by driving the input voltage signal to node v_{in1} and connecting nodes v_{in2} and v_{in3} to the ground

(iii) The high-pass biquad function can be realized from the proposed active filter designed in Figure 3 by driving the input voltage signal to node v_{in2} and connecting nodes v_{in2} and v_{in3} to the ground

(iv) The band-stop biquad function can be realized from the proposed active filter designed in Figure 3 by driving the input voltage signal to nodes $v_{in1}v_{in1}$ and v_{in2} and then connecting node v_{in3} to the ground

(v) The all-pass biquad function can be realized from the proposed active filter designed in Figure 3 by driving the input voltage signal to nodes v_{in1} and v_{in1} and driving the inverting input voltage signal to node v_{in3}. An inverting amplifier with unity gain is required for the all-pass function.

It is found from the above statement that the presented multifunction active filter designed in Figure 3 can provide five responses, named band-pass filter, low-pass filter, high-pass filter, band-stop filter, and all-pass filter, in the same circuit without the need for the double gain amplifier and the passive element matching condition. Moreover, the selection of the output voltage-mode filtering functions can be done by the digital approach employing a microcontroller or microprocessor.

In the case of the all-pass function, the phase response is given as follows:

$$\theta_{AP} = -2\tan^{-1}\left(\frac{\omega g_{m2} C_1 R}{g_{m1} - \omega^2 C_1 C_2 R}\right). \quad (7)$$

Equation (7) indicates that the phase difference in the input and output waveform for the AP function is shifted from 0° at low frequencies to −360° at high frequencies with a flat amplitude response where the phase of the output voltage waveform lags the phase of the input voltage waveform.

3. Analysis and Study of the Parasitic Effects on the Proposed Filter

In this section, the effect of the LT1228 parasitic element on the performance of the presented voltage-mode versatile active filter designed in Figure 3 is analyzed and studied. The commercially available LT1228 IC with the parasitic elements at the LT1228 input and output terminals can be drawn in Figure 4. The capacitance and resistance connecting in parallel configuration appear at the high-impedance input and output terminals V_+ ($R_+//C_+$), V_- ($R_-//C_-$), and y ($R_y//C_y$) and the transresistance impedance $R_T//C_T$. The resistor r_x and r_w series at the low-impedance terminals x and w, respectively. The parasitic effect appeared in the proposed filer is depicted in Figure 5, where $Y_A = s(C_{+1} + C_{-2} + C_{y1} + C_{y2}) + G_{+1} + G_{-2} + G_{y1} + G_{y2}$, $Y_{-1} = sC_{-1} + G_{-1}$, $Y_{T1} = sC_{T1} + G_{T1}$, and $Y_{T2} = sC_{T2} + G_{T2}$. The frequency limitations at low frequencies of the proposed filter (especially for the BP and HP functions) mostly stem from the parasitic resistances at the first LT1228. Ideally, the first LT1228, R, and C_1 are constructed as the lossless inductance simulator. However, the parasitic resistances cause this sub-circuit to work as the lossy inductance simulator (series LR circuit). If i_{y1} is the current going through the lossy inductance simulator (Figure 5), then the relationship between i_{y1} and v_{in1} and v_A is as follows:

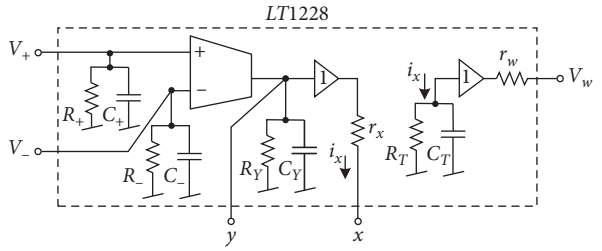

Figure 4: LT1228 parasitic elements.

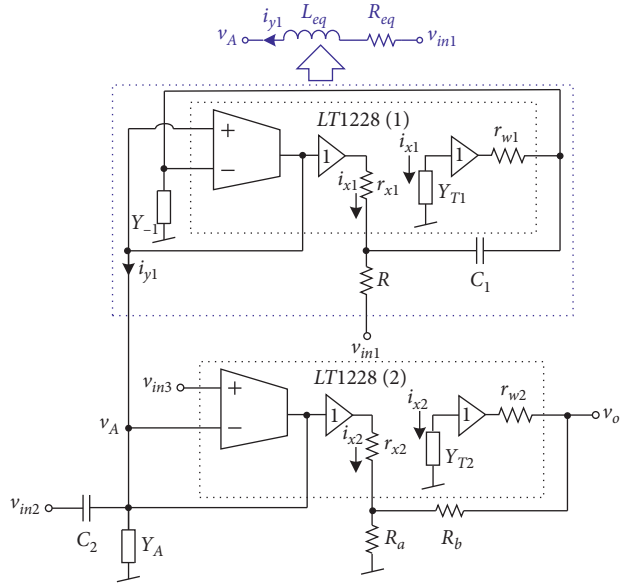

Figure 5: Proposed multifunction active filter with parasitic elements.

$$i_{y1} = \frac{1}{sL_{eq} + R_{eq}}\left[v_{in1} - v_A\left(sC_1R + 1 - R_{eq}g_{m1} - sL_{eq}g_{m1}\right)\right], \quad (8)$$

where

$$L_{eq} = \frac{C_1 R}{g_{m1}}\left[1 + \frac{r_{x1}}{R_{T1}}\left(1 + \frac{r_{w1}}{R_{-1}}\right) + \frac{r_{w1}}{R_{T1}}\left(1 + \frac{r_{x1}}{R}\right)\right], \quad (9)$$

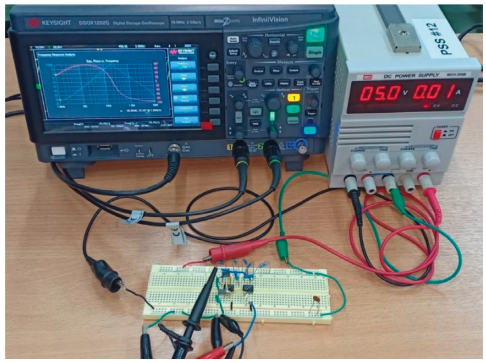

Figure 6: Experimental setup.

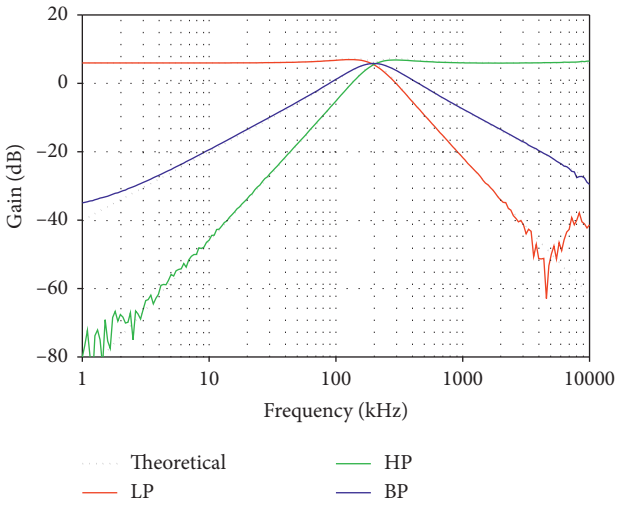

Figure 7: Experiment gain responses of LP, HP, and BP functions.

and

$$R_{eq} = \frac{r_{x1} r_{w1} R}{g_{m1} R_{T1} (r_{x1} // R)(r_{w1} // R_{-1})}. \quad (10)$$

From equation (10), the frequency limitations at low frequencies of the proposed filter (especially for the BP and HP functions) stem from the resistance, R_{eq}. To reduce this effect at low frequencies, the value of the external resistor, R, should be low. However, if R_{T1} and R_{-1} are greater than r_{x1}, r_{w1}, and R, then $R_{eq} \cong 0$ and $L_{eq} \cong C_1 R / g_{m1}$. The effect of the parasitic resistances at the first LT1228 is negligible (we also want to shorten the equation of the output voltage too).

At high frequencies, there are two poles/zeros (we will consider them as the poles) that appear at the inductance simulator. If r_{w1} is more less than R_{-1} and r_{x1} is more less than R_{T1}, these pole frequencies are $f_{p1} \cong 1/(2\pi C_{-1} r_{w1})$ and $f_{p2} \cong 1/(2\pi C_{T1} r_{x1})$. The CFA in the second LT1228, R_a, and R_b is constructed as the voltage amplifier. If R_{T2} is greater than r_{x2}, r_{w2}, and R_a, the bandwidth of the amplifier is determined by $1/(2\pi C_{T2} R_b)$ [47]. From the simulation in [47], it is

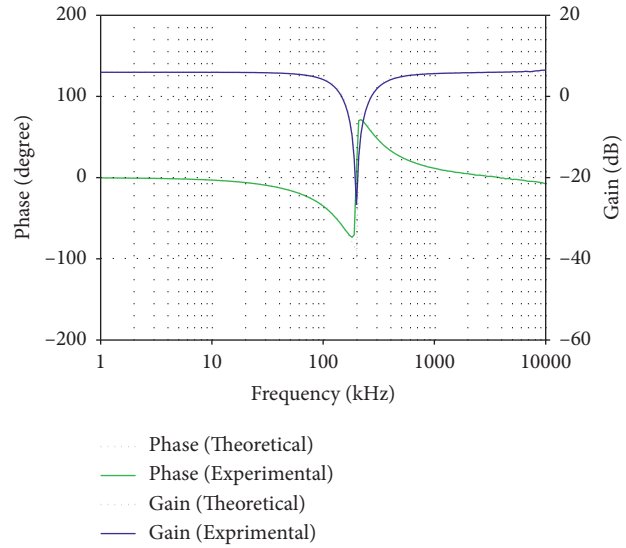

Figure 8: Experiment gain response of band-stop function.

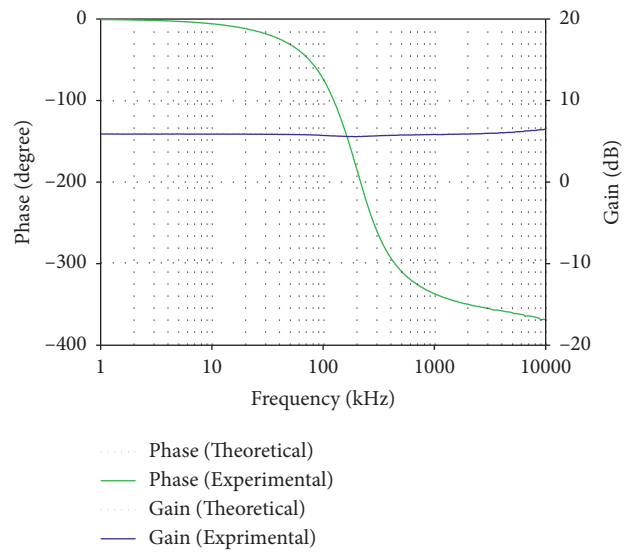

Figure 9: Experiment gain and phase response of all-pass function.

indicated that $C_y = 6$ pF, $R_y = 8$ MΩ, $C- = C_+ = 3$ pF, RT = 197.66 kΩ, CT = 5.95 pF, rx = 46.92 Ω, and $r_w = 19.80$ Ω [47]. If R_b and C_1 used in the proposed circuit are 1 kΩ and 1 nF, the pole frequencies, f_{p1} and f_{p2}, and bandwidth of the amplifier are approximately 2.68 GHz, 570.09 MHz, and 26.75 MHz, respectively. Thus, if the bandwidth of the proposed filter is less than 26.75 MHz, the effect of the parasitic elements, C_{-1}, R_{-1}, C_{T1}, R_{T1}, r_{w1}, and r_{x1} at the first LT1228 and R_{T2}, C_{T2}, r_{x2}, and r_{w2} at the second LT1228, is neglected. So, the most effect is caused by the parasitic elements, C+1, R+1, Cy1, Ry1, C−2, R−2, Cy2, and Ry2. Thus, the output voltage of the presented multifunction active filter with parasitic elements is obtained by

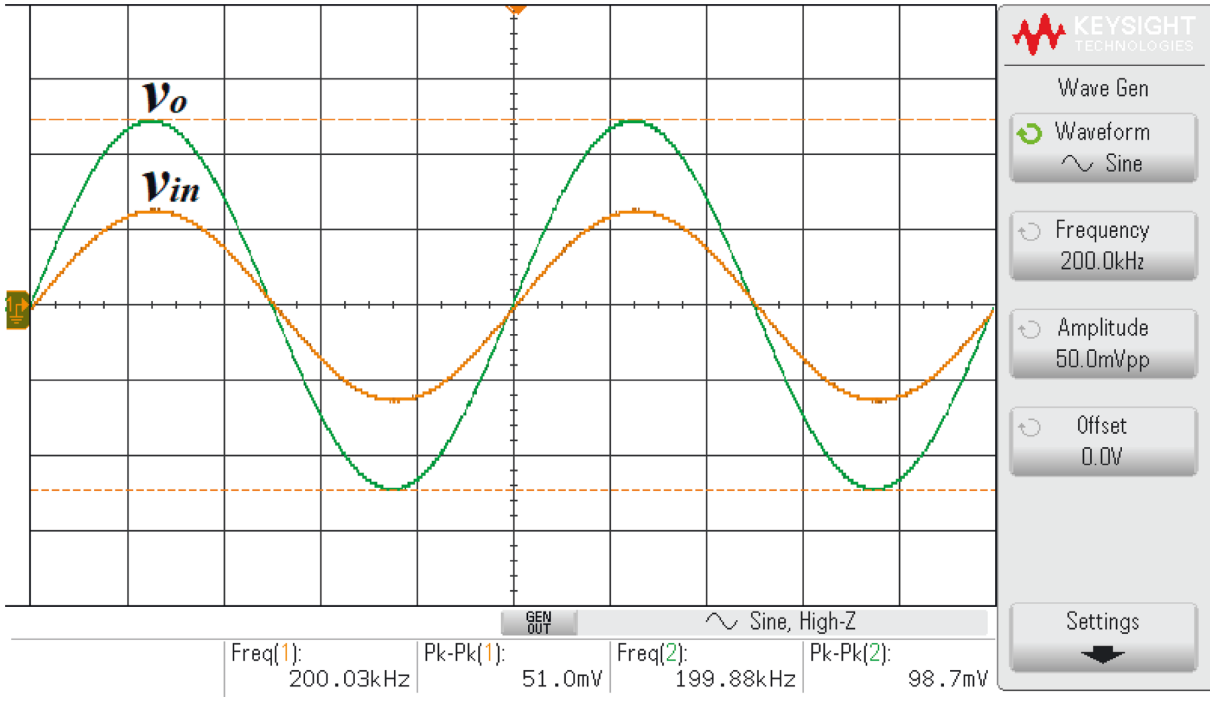

Figure 10: Measured input and output waveform of the BP filter.

$$v_o = \left(\frac{R_b}{R_a} + 1\right)\left[\frac{s^2(C_2/C_2 + C_A)v_{in2} + s(g_{m2}/C_A + C_2)v_{in3} + (g_{m1}/C_1R(C_A + C_2))v_{in1}}{s^2 + s(G_A + g_{m2}/C_A + C_2) + (g_{m1}/C_1R(C_A + C_2))}\right], \tag{11}$$

where $C_A = C_{+1} + C_{-2} + C_{y1} + C_{y2}$ and $G_A = G_{+1} + G_{-2} + G_{y1} + G_{y2}$. From equation (11), the natural frequency with the parasitic effect is given as follows:

$$\omega_0^* = \sqrt{\frac{g_{m1}}{C_1R(C_A + C_2)}}. \tag{12}$$

Subsequently, the quality factor with the parasitic effect is given as follows:

$$Q^* = \frac{1}{G_A + g_{m2}}\sqrt{\frac{g_{m1}(C_A + C_2)}{C_1R}}. \tag{13}$$

It is observed that the parasitic elements in the LT1228 affect the passband gain, phase response, natural frequency, quality factor, and the operating limitations at low and high frequencies. As discussed above, the value of the external resistor, R, should be low to reduce the parasitic effect at low frequencies. Also, the external resistor R_b should be low to enhance the bandwidth of the proposed circuit. In addition, to control the passband voltage gain with constant bandwidth, the value of R_a should be adjusted [47].

4. Experiment and Simulation Results

The proposed filter is verified with the hardware setup as depicted in Figure 6. The experiment is carried out using the supply voltages ±5 V. The filter is designed to obtain $f_0 = 200$ kHz, $Q = 1$, and the passband $G_p = 2$ by choosing $I_{B1} = 157.91\,\mu$A, $I_{B2} = 125.66\,\mu$A, $R = R_a = R_b = 1$ kΩ, and $C_1 = C_2 = 1$ nF. The magnitude frequency response of the proposed active filter for the functions, LP, HP, and BP filter, obtained from the experiment is illustrated in Figure 7. The experimental result shows $f_0 = 199.53$ kHz (0.23% error) and $Q = 1.05$ (5% error). The passband voltage gains of the proposed active filter for the functions, LP, HP, and BP filter, obtained from the experiment are 5.95 dB (1.16% error), 5.92 dB (1.66% error), and 5.79 dB (3.82% error), respectively. The magnitude and phase frequency response of the band-stop filtering function obtained from the experiment is depicted in Figure 8. The experimental passband voltage gains of the band-stop function at low and high frequencies are 5.95 (1.16% error) and 5.92 (1.66% error), respectively. The error of the experimental filtering parameters is caused by the parasitic resistances and capacitances in the commercial LT1228 IC as analyzed and discussed in Section 3.

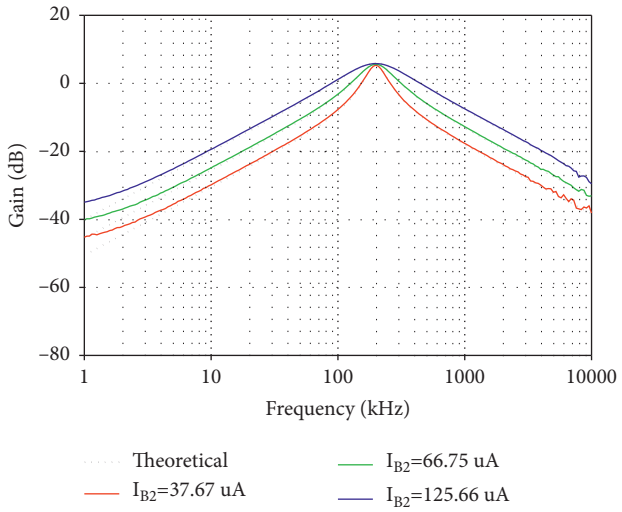

Figure 11: Experimental magnitude frequency response of BP function when I_{B2} is varied.

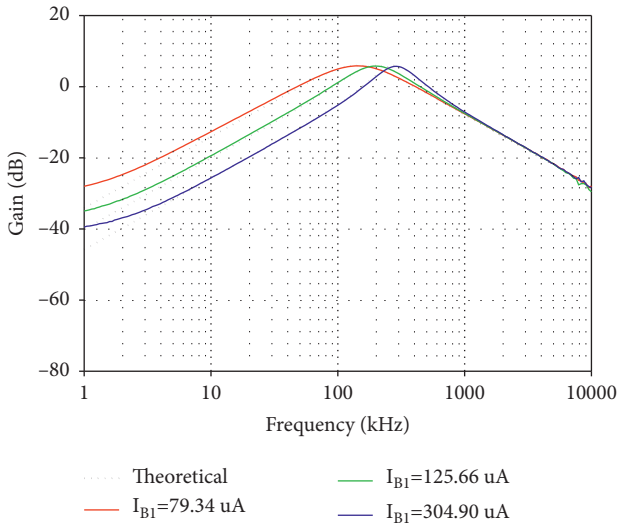

Figure 12: Experimental magnitude frequency response of BP function when I_{B1} is varied.

The gain and phase frequency behavior of the AP function obtained is depicted in Figure 9. The inverting unity gain amplifier is implemented by AD844 and two resistors (0.47 kΩ). It is seen that the phase behavior of the AP function is shifted from 0° at low frequencies to -360° at high frequencies with a flat amplitude response. The measured sinusoidal input and output waveform of the BP filter is illustrated in Figure 10, where the frequency of the sinusoidal input voltage is 200 kHz @ 50mVp-p. It is found that the sinusoidal input and output voltage signals are in phase at the center frequency ($f = 200$ kHz), while the BP output voltage is 98.7 $mV_{p\text{-}p,}$ which is around twice as large as the input. The total harmonic distortion (THD) of the BP output voltage is 0.191%. As expected in equation (5), the control of

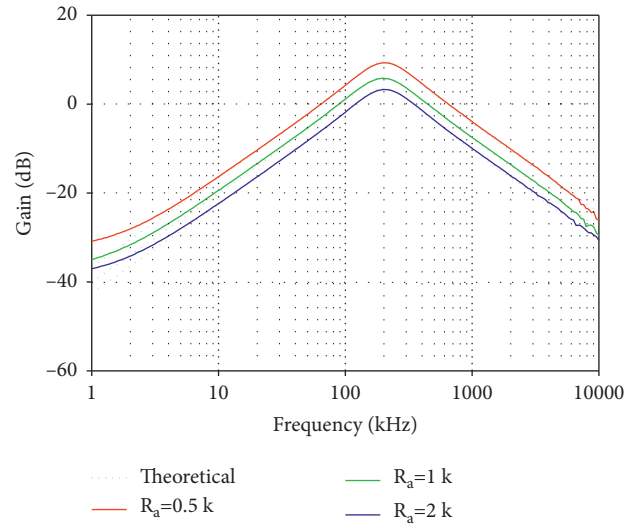

Figure 13: Experimental magnitude frequency response of BP function when R_a is varied.

the Q is done without affecting the f_0 by setting I_{B2} to 37.67 μA, 66.75 μA, and 125.66 μA ($I_{B1} = 157.91$ μA). This advantageous feature is confirmed by the experimental result in Figure 11. The experimental quality factors obtained from these values of I_{B2} are, respectively, varied to 2.69, 2.15, and 1.05. From the experimental result in Figure 12, changing I_{B1} to 79.34 μA, 125.66 μA, and 304.90 μA ($I_{B2} = 125.66$ μA) results in the natural frequency changing to 144.54 kHz, 199.53 kHz, and 288.40 kHz, respectively. However, adjusting I_{B1} will also affect the quality factor. So, in the practical design step, the natural frequency should be first tuned electronically by I_{B1}, and then, the bandwidth or the Q is electronically adjusted through I_{B2}. As mentioned in Section 3, the frequency limitation at high frequency of the proposed filter depends on the resistor, R_b. So, to control the passband voltage gain with constant bandwidth, the value of R_a should be adjusted [47]. The control of passband gain is experimentally verified via the BP function by adjusting the value of R_a to 0.5 kΩ, 1 kΩ, and 2 kΩ, respectively ($R_b = 1$ kΩ), as depicted in Figure 13. The experimental passband gains for these R_a values are 9.30 dB (2.52% error), 5.79 dB (3.82% error), and 3.27 dB (7.10% error), respectively. It is found that at a high value of R_a, the voltage gain error is quite high. So, the R_b can be decreased (R_a must be decreased too) to get a higher voltage gain. Also, if R_b is set to a low value, it can make the proposed circuit's bandwidth wider. The experimental result confirms that the passband gain is controllable as expected in equation (6). The step response of the low-pass filter is shown in Figure 14 for an input step amplitude of 50 mVp-p ($f = 15$ kHz).

In addition, the PSpice software is used to evaluate the performance of the proposed multifunction active filter. The macro-model of PSpice is at level 3. The input dynamic range of the proposed filter is evaluated by testing the THD of the output voltage versus the amplitude of the input voltage for band-pass filtering functions. Figure 15 depicts the

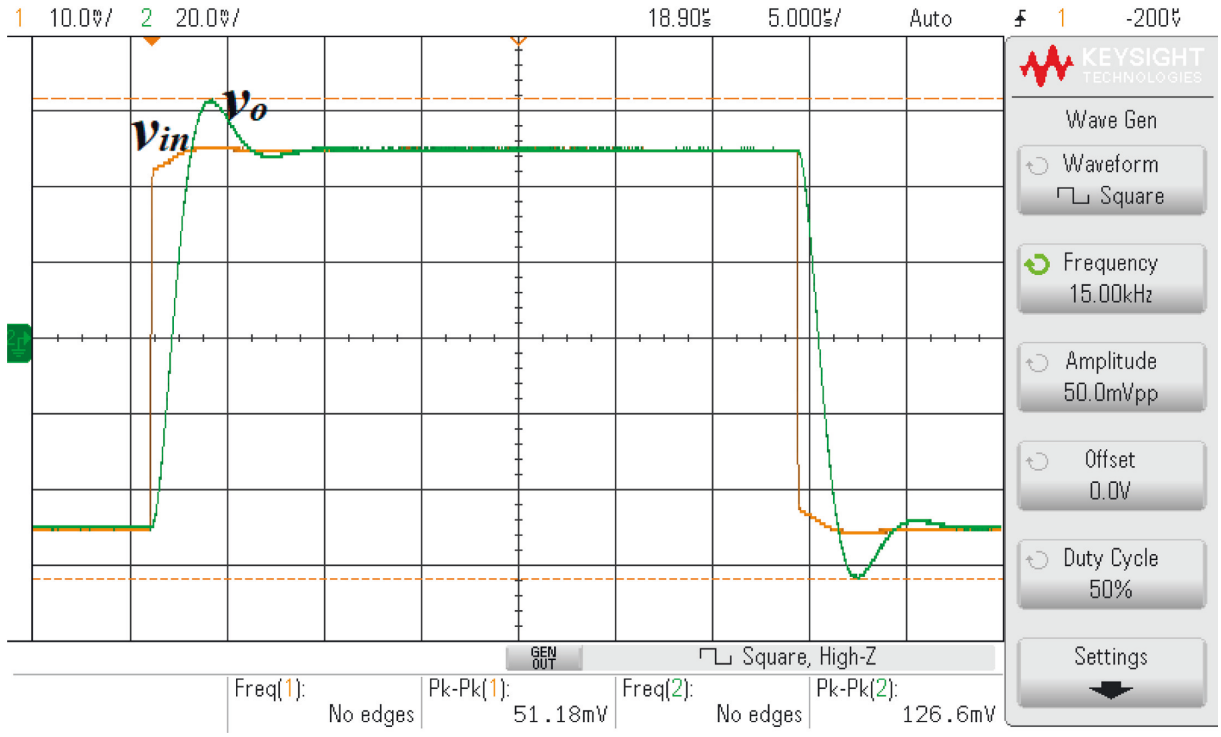

Figure 14: Measured input and output waveform of LP filter.

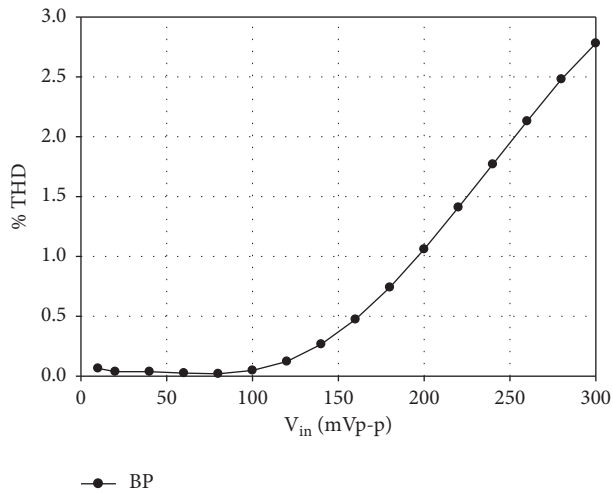

Figure 15: Simulated THD of the band-pass filter versus the input amplitude at $f = 200$ kHz.

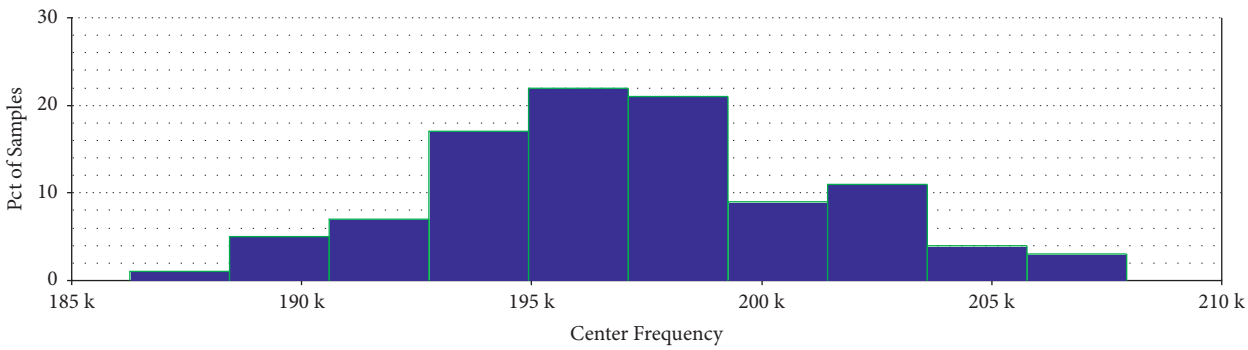

Figure 16: Histogram of Monte Carlo analysis of the band-pass filter with a ±5% passive element tolerance.

dependence of THD on the amplitude of the sinusoidal input voltage signal obtained through simulation, where the frequency of the sinusoidal input signal was 200 kHz. When the input voltage is less than 180 $mV_{p\text{-}p}$, the THD of the band-pass filtering function falls below 1 percent. The band-pass function of the proposed multifunction filter is analyzed using the Monte Carlo method to examine the influence of passive elements on the performance of the circuit. In this simulation, the Gaussian variation of the resistance and capacitance is 5%, while the other active elements are identical to those observed in the previous experiment. Statistical analysis is performed on the Monte Carlo 100 simulation. After 100 runs, the band-pass filter's center frequency varies between 186.26 kHz and 207.93 kHz, with a standard deviation of 4247.02 Hz as depicted in Figure 16.

5. Conclusions

In this design, the voltage-mode versatile biquadratic filter with amplitude controllability using the commercially available LT1228 ICs is proposed. The proposed filter contains two LT1228 ICs, three resistors (R, R_a, and R_b), and two capacitors (C_1 and C_2). The low-impedance output voltage node of the proposed circuit is achieved, which is able to connect to other circuits without the need for external buffer circuits. Five standard filter responses, including HP, BP, BS, LP, and AP filtering functions, can be obtained in the same core filtering structure without any matching conditions and a double gain amplifier. With this advantage feature, the filtering function of the proposed versatile active filter can be chosen by the digital approach. Both parameters (f_0 and Q) can be electronically adjusted by I_{B1} and I_{B2}. Moreover, Q can be tuned by the bias current, I_{B1}, without affecting the parameter, f_0. The passband gain is controllable by adjusting the resistors R_a and R_b without disturbing the parameters, Q and f_0. However, the inverting unity gain amplifier is required for the AP filtering function. The input voltage nodes, v_{in2} and v_{in1}, are not high impedance. The simulation results from the PSpice program and experiment results from the hardware test are carried out to investigate the proposed multifunction active filter. With the supply voltages ±5 V and choosing $I_{B1} = 157.91\,\mu A$, $I_{B2} = 125.66\,\mu A$, $R = R_a = R_b = 1\,k\Omega$, and $C_1 = C_2 = 1$ nF, the natural frequency obtained from the experiment is 199.53 kHz (0.23% error). The quality factor obtained from the experiment is 1.05 (5% error).

Data Availability

No data were used to support the findings of this study.

Conflicts of Interest

The authors declare that they have no conflicts of interest.

Acknowledgments

This work was supported by King Mongkut's Institute of Technology Ladkrabang (KREF016301).

References

[1] L. Safari, G. Barile, G. Ferri, and V. Stornelli, "High performance voltage output filter realizations using second generation voltage conveyor," *International Journal of RF and Microwave Computer-Aided Engineering*, vol. 28, 2018.

[2] M. T. Abuelma'atti and N. R. Almutairi, "New current-feedback operational-amplifier based shadow filters," *Analog Integrated Circuits and Signal Processing*, vol. 86, pp. 471–480, 2016.

[3] R. Gupta and S. S. Gupta, "New universal filter using only current followers as active elements," *AEU - International Journal of Electronics and Communications*, vol. 60, no. 3, pp. 251–256, 2006.

[4] R. Senani, V. K. Singh, A. K. Singh, and D. R. Bhaskar, "Novel electronically controllable current-mode universal biquad filter," *IEICE Electronics Express*, vol. 1, no. 14, pp. 410–415, 2004.

[5] N. Pandey and S. K. Paul, "Differential difference current conveyor transconductance amplifier: a new analog building block for signal processing," *Journal of Electrical and Computer Engineering*, vol. 2011, Article ID 361384, 2011.

[6] G. Barile, L. Safari, L. Pantoli, V. Stornelli, and G. Ferri, "Electronically tunable first order AP/LP and LP/HP filter topologies using electronically controllable second generation voltage conveyor (CVCII)," *Electronics*, vol. 10, no. 7, p. 822, 2021.

[7] M. T. Abuelma, atti, and A. Bentrcia, "A new mixed-mode OTA-C filter/oscillator circuit," *Journal of Active and Passive Electronic Devices*, vol. 3, pp. 211–221, 2008.

[8] B. Singh, A. K. Singh, and R. Senani, "A new universal biquad filter using differential difference amplifiers and its practical realization," *Analog Integrated Circuits and Signal Processing*, vol. 75, no. 2, pp. 293–297, 2013.

[9] R. Senani, D. R. Bhaskar, and P. Kumar, "Two-CFOA-grounded-Capacitor first-order all-pass filter configurations with ideally infinite input impedance," *AEU - International Journal of Electronics and Communications*, vol. 137, Article ID 153742, 2021.

[10] M. T. Abuelma'atti, S. K. Dhar, and Z. J. Khalifa, "New two-CFOA-based floating immittance simulators," *Analog Integrated Circuits and Signal Processing*, vol. 91, pp. 479–489, 2017.

[11] V. Stornelli, G. Barile, L. Pantoli et al., "A new VCII application: sinusoidal oscillators," *Journal of Low Power Electronics and Applications*, vol. 11, no. 3, p. 30, 2021.

[12] S. Maheshwari and M. S. Ansari, "Catalog of realizations for DXCCII using commercially available ICs and applications," *Radioengineering*, vol. 21, pp. 281–289, 2012.

[13] E. Minaei and S. Minaei, "Realization of arbitrary current transfer functions based on commercially available CCII + s," *International Journal of Circuit Theory and Applications*, vol. 42, no. 7, pp. 659–670, Jul 2014.

[14] S. Jaikla and W. Jaikla, "Electronically controllable grounded inductance simulators using single commercially available IC: LT1228," *AEU - International Journal of Electronics and Communications*, vol. 76, pp. 1–10, 2017.

[15] M. Kumngern, M. Somdunyakanok, and P. Prommee, *High-Input Impedance Voltage-Mode Multifunction Filter with Three-Input Single-Output Based on Simple CMOS OTAs*, IEEE, Vientiane, Laos, 2008.

[16] J.-W. Horng, "High input impedance voltage-mode universal biquadratic filter using two OTAs and one CCII," *International Journal of Electronics*, vol. 90, no. 3, pp. 185–191, 2003.

[17] C. Lee and M.-S. Lee, "Universal voltage-mode filter with three inputs and one output using three current conveyors and one voltage follower," *Electronics Letters*, vol. 30, no. 25, pp. 2112-2113, 1994.

[18] J.-W. Horng, C.-C. Tsai, and M.-H. Lee, "Novel universal voltage-mode biquad filter with three inputs and one output using only two current conveyors," *International Journal of Electronics*, vol. 80, no. 4, pp. 543–546, 1996.

[19] J.-W. Horng, M.-H. Lee, H.-C. Cheng, and C.-W. Chang, "New CCII-based voltage-mode universal biquadratic filter," *International Journal of Electronics*, vol. 82, no. 2, pp. 151–156, 1997.

[20] C.-M. Tu and S.-H. Tu, "Universal voltage-mode filter with four inputs and one output using two CCII s," *International Journal of Electronics*, vol. 86, no. 3, pp. 305–309, 1999.

[21] J.-W. Horng, "Voltage-mode universal biquadratic filters using CCIIs," *IEICE - Transactions on Fundamentals of Electronics, Communications and Computer Sciences*, vol. E87A, pp. 406–409, 2004.

[22] A. Ranjan and S. K. Paul, "Voltage mode universal biquad using CCCII," *Active and Passive Electronic Components*, vol. 2011, Article ID 439052, 2011.

[23] N. Herencsar, J. Koton, and K. Vrba, "Single CCTA-based universal biquadratic filters employing minimum components," *International Journal of Computer and Electrical Engineering*, vol. 1, pp. 307–310, 2009.

[24] J. K. Pathak, A. K. Singh, and R. Senani, "New voltage mode universal filters using only two CDBAs," *ISRN Electronics*, vol. 2013, Article ID 987867, 2013.

[25] J.-W. Horng, "Voltage-mode multifunction filter using one current feedback amplifier and one voltage follower," *International Journal of Electronics*, vol. 88, no. 2, pp. 153–157, 2001.

[26] C.-M. Chen and H.-P. Chen, "Universal capacitor-grounded voltage-mode filter with three inputs and a single output," *International Journal of Electronics*, vol. 90, no. 6, pp. 401–406, 2003.

[27] W. Horng and J. Horng, "High-input and low-output impedance voltage-mode universal biquadratic filter using DDCCs," *IEEE Transactions on Circuits and Systems II: Express Briefs*, vol. 54, no. 8, pp. 649–652, 2007.

[28] N. A. Malik and M. A. Malik, "Voltage/current-mode universal filter using FTFN and CFA," *Analog Integrated Circuits and Signal Processing*, vol. 45, no. 2, pp. 197–203, 2005.

[29] C.-M. Chen and H.-P. Chen, "Single FDCCII-based tunable universal voltage-mode filter," *Circuits, Systems, and Signal Processing*, vol. 24, no. 2, pp. 221–227, 2005.

[30] C. Hua-Pin and L. Yi-Zhen, "High-input and low-output impedance voltage-mode universal biquadratic filter using FDCCIIs," in *Proceedings of the 2008 9th International Conference on Solid-State and Integrated-Circuit Technology*, pp. 1794–1798, IEEE, Beijing, China, October 2008.

[31] S. Kilinç, A. U. Keskin, and U. Çam, "Cascadable voltage-mode multifunction biquad employing single OTRA," *Frequenz*, vol. 61, pp. 84–86, 2007.

[32] I. Myderrizi, S. Minaei, and E. Yuce, "DXCCII-based grounded inductance simulators and filter applications," *Microelectronics Journal*, vol. 42, no. 9, pp. 1074–1081, 2011.

[33] J. Satansup and W. Tangsrirat, "Single VDTA-based voltage-mode electronically tunable universal filter," in *Proceedings of the 27th International Technical Conference on Circuits/Systems, Computers and Communications ITC-CSCC 2012*, Hokkaido, Japan, July 2012, https://conference.researchbib.com/?action=viewConferenceSearch&country=jp.

[34] W. Tangsrirat and O. Channumsin, "Voltage-mode multifunctional biquadratic filter using single DVCC and minimum number of passive elements," *Indian Journal of Pure and Applied Physics*, vol. 49, pp. 703–707, 2011.

[35] C. L. Hou, C. C. Huang, Y. S. Lan, J. J. Shaw, and C. M. Chang, "Current-mode and voltage-mode universal biquads using a single current-feedback amplifier," *International Journal of Electronics*, vol. 86, no. 8, pp. 929–932, 1999.

[36] K. L. Pushkar, D. R. Bhaskar, and D. Prasad, "A new MISO-type voltage-mode universal biquad using single VD-DIBA," *ISRN Electronics*, vol. 2013, Article ID 478213, 2013.

[37] S. Jaikla and W. Jaikla, "Universal filter using single commercially available IC: LT1228," *MATEC Web of Conferences*, vol. 95, Article ID 14002, 2017.

[38] S. Sangyaem, S. Siripongdee, W. Jaikla, and F. Khateb, "Five-inputs single-output voltage mode universal filter with high input and low output impedance using VDDDAs," *Optik*, vol. 128, pp. 14–25, 2017.

[39] P. Supavarasuwat, M. Kumngern, S. Sangyaem, W. Jaikla, and F. Khateb, "Cascadable independently and electronically tunable voltage-mode universal filter with grounded passive components," *AEU - International Journal of Electronics and Communications*, vol. 84, pp. 290–299, 2018.

[40] A. Chaichana, S. Sangyaem, and W. Jaikla, "Multifunction voltage-mode filter using single voltage differencing differential difference amplifier," *MATEC Web of Conferences*, vol. 95, Article ID 14003, 2017.

[41] S. Siripongdee and W. Jaikla, "Single VDDDA-based voltag-mode multifunction second order filter for analog signal processing," in *Proceedings of the 2015 International Conference on Intelligent Informatics and Biomedical Sciences (ICIIBMS)*, Okinawa, Japan, November 2015.

[42] J. Pimpol, O. Channumsin, and W. Tangsrirat, "MISO universal filter employing single VDTA," in *Proceedings of the 2018 International Conference on Engineering, Applied Sciences, and Technology (ICEAST)*, pp. 1–4, IEEE, Langkawi, Malaysia, September 2011.

[43] M. Kumngern and U. Torteanchai, "Voltage-mode MISO OTA-C biquad filter," in *Proceedings of the 2011 IEEE Symposium on Industrial Electronics and Applications*, pp. 79–82, IEEE, Langkawi, Malaysia, September 2011.

[44] P. Suwanjan, S. Siripongdee, and W. Jaikla, "Three-inputs single-output voltage-mode universal filter with orthogonal control using single commercially available IC," in *Proceedings of the 2017 European Conference on Electrical Engineering and Computer Science (EECS)*, pp. 454–457, IEEE, Bern, Switzerland, November 2017.

[45] S. Klungtong, D. Thanapatay, and W. Jaikla, "Three-input single-output voltage-mode multifunction filter with electronic controllability based on single commercially available IC," *Active and Passive Electronic Components*, vol. 2017, Article ID 5240751, 2017.

[46] LT1228, "100MHz Current Feedback amplifier with DC gain control," Linear techonology, CA, USA, 2012, https://www.analog.com/media/en/technical-documentation/data-sheets/1228fd.pdf.

[47] W. Jaikla, U. Buakhong, S. Siripongdee et al., "Single commercially available IC-based electronically controllable voltage-mode first-order multifunction filter with complete standard functions and low output impedance," *Sensors*, vol. 21, no. 21, p. 7376, 2021.